Experimental study of airflow and heat transfer above a hot liquid surface simulating a cup of drink

Onrawee Laguerre, Véronique Osswald, Hong-Minh Hoang, Isabelle I. Souchon, Ioan-Cristian Trelea, Christoph Hartmann, Denis Flick

Experimental study of airflow and heat transfer above a hot liquid surface simulating a cup of drink

O. Laguerre[a]✉, V. Osswald[a], H.M. Hoang[a], I. Souchon[bc], C.Trelea[bc], C. Hartmann[d], D. Flick[e]

[a] Irstea, UR GPAN, 1 rue Pierre-Gilles de Gennes, 92761 Antony, France

[b] INRA, UMR782 GMPA, 78850 Thiverval Grignon, France

[c] AgroParisTech, UMR782 GMPA, 78850 Thiverval Grignon, France

[d] Nestlé Research Center, CH-1000 Lausannen, Switzerland

[e] AgroParisTech, UMR Ingénierie Procédés Aliments, AgroParisTech, INRA, Université Paris Saclay, F-91300 Massy, France

Abstract

This work was carried out to study the airflow and heat transfer above a cup of hot drink. The experiment was undertaken in a device in which the air temperature and velocity were controlled representing a room condition. The influence of heat exchange by convection and evaporation between the hot drink (at different temperatures) and air on the velocity and temperature fields above the cup is presented. An experimental methodology was developed to evaluate the heat transfer coefficient between the air and hot drink with and without evaporation.

The airflow visualisation by PIV (Particle Imagery Velocimetry) above the cup shows that the flow is complex with unsteady plumes detachment and vortex formation. The combined convection and evaporation lead to upward airflow with temperature fluctuations which become significant for drink temperature above 55°C. This can be explained by the non-

✉ Corresponding author: Tel: 33 1 40 96 61 21 Fax: 33 1 40 96 60 75 E-mail: onrawee.laguerre@irstea.fr

linearity between saturated pressure of water and its temperature. This work could highlight how volatile aromas are released from hot drink.

Keywords: convection, evaporation, airflow, hot drink, air

Nomenclature

A	surface area	m^2
D	cylinder diameter	m
L	characteristic length	m
f	frequency of vortex shedding	Hz
g	gravitational acceleration	$m.s^{-2}$
h	convective heat transfer coefficient	$W.m^{-2}.K^{-1}$
M	molecular weight	kg/mol
Q	heat exchange	W
t	time	s
T	temperature	°C
v	velocity	$m.s^{-1}$
x	molar fraction of water in air	

Greek symbols

β	thermal expansion coefficient	K^{-1}
ρ	density of the fluid	$kg.m^{-3}$

ν	kinematic viscosity	$m^2.s^{-1}$
α	thermal diffusivity	$m^2.s^{-1}$

30

31 **Dimensionless Number**

Reynolds number $Re_L = \frac{v_\infty L}{\nu}$	Characterization of flow regimes for forced convection: laminar or turbulent flow
Grashof number $Gr_L = \frac{g\beta(T_w - T_\infty)L^3}{\nu^2}$	Ratio of buoyancy to viscous force acting on a fluid
Prandt number $Pr = \frac{\nu}{\alpha} = 0.71$ for air	Ratio of momentum diffusivity to thermal diffusivity
Rayleigh number $Ra_L = Gr_L . Pr_L$	Characterization of flow regime for natural convection: laminar or turbulent flow
Nusselt number $Nu_L = \frac{h.L}{\lambda_{air}}$	Ratio of convective to conductive heat transfer
Richardson number $Ri_L = \frac{Gr_L}{Re_L^2}$	Characterization of the importance of natural convection relative to forced convection

Strouhal number $St = \frac{fD}{v}$	Dimensionless frequency of oscillating flow

I. Introduction

Odour during food consumption largely influences perception of foods and is thus determinant in consumer preference. Food aroma compounds are released to ambient air and are responsible for the ambient smell of the room where the food is consumed. The ambient smell greatly influences food intake and food choice (Stroebele and De Castro, 2004). To be able to better understand the impact of smell ambient due to food on consumer behaviour, it is first necessary to identify key room factors impacting aroma release to ambient air. Aroma release phenomena involve multi-factorial and complex processes. In the case of a cup of hot drink, it consists in aroma diffusion to liquid surface, aroma transportation to the surrounding air due to diffusion, convection and compounds/water mixture evaporation through a boundary layer (located above liquid surface). Then, aroma compounds follow airflow in the room and arrive to the consumer nose. This study focuses only on the airflow, heat and vapour transfer just above the cup. The understanding of these mechanisms is a first step useful for understanding and controlling the aroma perception by consumer.

1.1. Studies on aroma compounds in foods

Aroma, which is one of the key components of food flavour, depends on the type and concentration of volatile compounds present in the air above the food and in the oral cavity during eating, and how they interact with appropriate sensory receptors in nose when they are carried by the breath of the individual (Overbosch et al., 1991; Taylor and Linforth, 1996).

53 Many studies highlighted the influence of physicochemical properties of aroma compounds
54 (volatility, hydrophobicity), the released amounts and kinetics, for model food (Landy et al.,
55 1998; Marin et al., 1999, Carey et al., 2002; Philippe et al., 2003; Rabe et al., 2004; Meynier
56 et al., 2005; Giroux et al., 2007) and real food (Doulia et al., 2000; Doyen et al., 2001;
57 Roberts et al., 2003; Relkin et al., 2004, Deleris et al., 2009). In the case of real food, products
58 are generally complex. Thus, global characterization and determination of apparent properties
59 are often the most convenient ways to represent transport properties and explain release
60 profiles. For solid foods, aroma release is often limited by the diffusion inside the food. For
61 liquid foods, especially drinks of low viscosity, release is also controlled by the transport
62 phenomena from the liquid/air interface to surrounding air (Marin et al, 1999).

63

64 **1.2. Airflow and heat transfer between object and air**

65 The exchange between the hot drink and the ambient air can be due to natural or forced
66 convection. To understand the airflow, heat and water transfer between a cup of hot drink and
67 air, the simplest way is to consider the similar phenomena occurring above a heated horizontal
68 flat plate. Another way is to consider the cup as a cylindrical obstacle of airflow. A literature
69 review of air flows over a flat plate and around a cylinder is, thus, presented below.

70 Over an isothermal flat plate, a laminar flow is first observed, then after a certain flow length
71 (called critical length) the flow becomes unstable and turbulent. This instability occurs usually
72 when $\mathrm{Re} \approx 3.10^5$ (DeWitt, 1990).

73 Different flow patterns occur around a cylinder in function of air velocity. For Re<<1, the
74 flow smoothly divides and reunites around the cylinder. For $\mathrm{Re} \approx 10$, the flow separates in
75 the downstream and the wake is formed by two symmetric eddies. The eddies remain steady
76 and symmetrical but grow in size up to a Reynolds number of about 90. At $\mathrm{Re} \geq 90$, the

77 symmetry between the two eddies is broken. The downstream vortices become unstable,
78 separate from the body and are alternately shed downstream for $90 \le Re \le 10^4$. The alternate
79 shedding is called the Karman vortex street. This type of flow is unsteady but repeats itself at
80 some time interval. At about $10^4 \le Re \le 10^5$, the periodic flow breaks down into a chaotic
81 wake and tends to become turbulent. The Strouhal number (St) describes the unsteady,
82 oscillating flow mechanisms. For a long cylinder, and for $Re \le 800$ or $Re \ge 2.10^5$, St is a
83 function of the Reynolds number. For $800 \le Re \le 2.10^5$, St value is almost constant (~0.2)
84 which means that the frequency of vortex shedding is proportional to the air velocity (Hall,
85 2000).

86 For natural convection, the driving force is the temperature difference between the drink and
87 air, the flow regime is characterised by the Rayleigh number: Ra (warm air flows upward
88 from the drink surface and this air is replaced by cooler air flowing downward from the
89 ambient). For forced convection which may occur in ventilated room, the driving force is air
90 velocity, the flow regime is characterised by the Reynolds number Re. The intensity of heat
91 exchange is characterised by Nusselt number (Nu) which can be related to mass exchange by
92 Lewis analogy.

93 Incropera and Dewitt (1996) proposed the following correlations of the mean Nusselt number
94 ($\overline{Nu}_L$) for airflow over a horizontal flat plate of characteristic length L.

95 Natural convection, here L is the surface area divided by the perimeter:

$$\overline{Nu}_L = 0.54 Ra_L^{1/4} \quad 10^4 \le Ra_L \le 10^7 \qquad \text{Laminar flow} \qquad (1)$$

$$\overline{Nu}_L = 0.15 Ra_L^{1/3} \quad 10^7 \le Ra_L \le 10^{11} \qquad \text{Turbulent flow} \qquad (2)$$

96 Forced convection, here L is the length of the plate in the flow direction:

$$\overline{Nu}_L = 0.664\,Re_L^{1/2}\,Pr^{1/3} \quad Re_L \le 2500 \qquad \text{Laminar flow} \qquad (3)$$

$$\overline{Nu}_L = 0.037\,Re_L^{0.8}\,Pr^{1/3} \quad Re_L > 2500 \qquad \text{Turbulent flow} \qquad (4)$$

The Richardson number ($Ri = Gr/Re^2$) indicates the importance of natural convection relative to the forced convection. Typically, the natural convection is considered when $Ri>10$ (negligible forced convection), mixed convection when $0.1 < Ri < 10$ and forced convection is considered when $Ri<0.1$ (negligible natural convection) (Incropera and Dewitt, 1966).

Most of the studies found in the literature about fluid flow and heat transfer around complex obstacles are applied to building air conditioning, heat exchangers and electronic equipment cooling. In these applications, various obstacles are employed to alter the flow pattern and which leads to locally increase or decrease heat exchange. The experimental studies are rare in comparison with the numerical ones because of the metrology difficulties and cost. Several authors reported that the fluid flow over blocks is complicated unsteady motion and the average flow often looks very different from the instantaneous flow (Rahman et al, 2008; 2009; Chyu and Natarajan, 1996). Although the geometry has a symmetry plane, the instantaneous velocity field is not symmetric while the time average flow must be symmetric. Looking only the time-averaged flow may give an erroneous impression.

Wietrzak and Poulikakos (1990), Yong and Vafai (1998), Alamyane and Mohamad (2010), Moussaoui et al (2010) numerically studied the forced convection of a heated obstacle mounted on a channel wall. The characterisation of flow field surrounding the obstacle and the local Nusselt number (Nu) distribution were presented. It was shown that the obstacle height/width ratio, the thermal conductivity of solid and fluid ratio, the flow rate (Re number) and the heating method can produce significant effects on the flow characteristic and heat transfer coefficient. Increase in the obstacle height strengthened fluid recirculation before, after and upon the top surface of obstacle, thus increasing the Nusselt number. The changes in

obstacle size or shape can lead to Nusselt number increases as high as 40% (Jubran et al, 1996) and mass transfer enhancements up to two times (Sparrow et al. 1982, 1984). Heat transfer and airflow by mixed convection around a hollow cylinder placed in a ventilated cavity was studied by Mamun et al (2010). A wide range of pertinent parameters such as Rayleigh number (0-105), Richardson number (0.0-5.0), dimensionless cylinder diameter (0.2-0.5) and the solid-fluid thermal conductivity ratio (0.2-10.0) are considered for Reynolds number = 100. It is observed that the cylinder diameter has significant effect on both the flow and thermal fields but the solid-fluid thermal conductivity ratio has significant effect only on the thermal field. As our best knowledge, few studies were carried out in the case of partially hollow cylinder which corresponds to a cup partially filled with drink.

Our literature study has shown a lack of knowledge on the mechanism of the combined airflow, heat and water transfer around an obstacle applied to the case of a cup of hot drink. To complete this knowledge, this study was carried out. The objectives of this work were, firstly, to develop a methodology of measurement of air velocity field above a cup filled with hot water by PIV (Particle Imagery Velocimetry) and to study the influence of water temperature on air velocity field above the cup. Secondly, to measure the heat transfer coefficient between the water in the cup and the surrounding air. This coefficient determines the water temperature decreasing rate. It is to be reminded that two heat transfer modes take place between the water in the cup and the air: convection and evaporation. The natural convection is related to the temperature difference between water and air, forced convection has also to be considered if the ambient air circulates due to room ventilation. The final practical objective of this work is to optimize the serving manner and the cup design in such a way that the consumer perceives as much as possible the aroma of hot drink.

II. Material and Methods

144 **2.1. Experimental device**

145 To represent room condition, the experiment was carried out in a device specifically
146 developed for this study, in which the ambient temperature and velocity were controlled
147 (Figure 1). This device is composed of 2 parts. In the part 1, a honeycomb was used over a
148 cross section in order to avoid developing flow effects. In the part 2, the work zone was
149 equipped with two glass walls (front and top). Two fans located at the vertical right hand side
150 wall allow low air velocities in the work zone by air extraction. The work zone is equipped
151 with an anemometer (air velocity sensor), thermocouple (temperature sensor) and hygrometer
152 (air humidity sensor).

153

154 **2.2. Air velocity field measured by PIV (Particle Image Velocimetry)**

155 Oil smoke was use as tracer for the air velocity measurement by PIV. The diameter of smoke
156 particles (~1 μm, manufacturer data) is very small so that they follow the airflow.

157 Figure 2 shows the 2-Dimensional PIV system (LaVision Company). It is composed of CCD
158 camera (12 bits double matrices of 1376 x 1024 pixels) allowing the acquisition of 2 images
159 successively within a short time interval. The sequence of images taken by the camera is
160 synchronised with the 2 laser impulsions (4 couples of images per second). An instantaneous
161 air velocity field is obtained by inter-correlation of 2 successive images of smoke particles
162 presented in a strongly enlightened plan. In our case, a good velocity estimation could be
163 obtained with 6.5 ms between 2 laser pulses for the image dimension (width x height) of 7.2
164 cm x 8.7 cm. Vector calculation was undertaken from interrogate windows of dimension 32 x
165 32 pixels with 50% of overlap between windows. Thus, there are 16 pixels (~1 mm) between
166 2 calculated vectors in both horizontal and vertical directions. A mean velocity field was
167 calculated from 700 couples of images. These images were taken on the symmetry plane and

168 just above a black cup (height x diameter = 11 cm x 8 cm) filled with oil or water (10 cm
169 height). This is because the time average velocity vectors belong to this plan. In this way, the
170 effect of 3D pattern is reduced.

171

172 **2.3. Air temperature fluctuations measurement**

173 To avoid as much as possible the flow disturbance in horizontal direction (air flows by fan
174 aspiration ≈ 0.03 m/s) and in vertical one (air flows by natural convection and by evaporation)
175 because of the presence of thermocouples, calibrated T-type fine thermocouples (200 µm
176 diameter, precision ±0.2°C) were used to follow the air temperature fluctuations with time.
177 These thermocouples were tightened on a Plexiglas support (5 ± 0.1 mm space between
178 thermocouples shown in Fig. 3a). This support was placed at right angle to the airflow
179 direction to avoid the flow perturbation. Because of the very fine thermocouple diameter,
180 airflow was very slightly disturbed by their presence (the thermocouples occupy only 4% of
181 the flow cross-section). In our experiment, the air temperature was measured every second for
182 y varying from 5 mm to 40 mm from the top of the cup while x was fixed at 68.5mm (Fig.
183 3b).

184

185 **2.4. Experimental conditions**

186 The device was located in a test room with the controlled ambient temperature of 20°C
187 (relative humidity about 60%). The fan tension of 2.5V allowed obtaining an air velocity of
188 about 0.03 m/s in the work zone which is the order of magnitude of the one in a room (Plana-
189 Fattori et al., 2014). During experiment, the air velocity near the entrance of the work zone
190 was measured using an anemometer to assure that it was not modified because of the presence
191 of the cup.

In order to study the influence of convection and evaporation on the airflow, the air velocity field was measured (using PIV) above a cup filled with vegetable oil (boiling temperature 165°C) and with water. The temperature of the oil was controlled at 20°C or 65°C. The temperature of water was controlled at several temperatures varying from 35 to 65°C (temperature of hot drink in general) using a heating resistance. An experiment was also carried out without any cup.

2.5. Measurement of convective heat transfer coefficient

The convective heat transfer coefficient between the liquid in the cup and air was measured in the work zone (Figure 4). The liquid (oil or water) in the cup was heated by a resistance (supply power: Q) until 65°C ±1°C and this temperature was maintained during the measurement (steady state). Once the steady state was reached, the air and liquid temperatures (T_{air}, T_{liq} respectively) were recorded every 10s for about 50min using a data logger, and then the mean values were calculated. Two conditions were used: cup covered with an insulating plate made of polystyrene (8 cm diameter, 1 cm thickness, Figure 4a) and un-covered cup (Figure 4b). In the case of un-covered cup, the weight of the cup before and after experiment was recorded in order to obtain the weight of evaporated water (Δm).

It is to be reminded that the convective heat transfer coefficient is an average value over the whole liquid surface. This coefficient determined at the liquid/air interface (h) can be calculated by the following manner:

Cup covered with insulating plate

This experiment was carried out in order to quantify heat losses through the cup's wall (Q_{loss}) while the heat loss through the insulating plate was neglected. At steady state, the heating power supply to the resistance (Q_1) is equal to the heat losses.

Un-covered cup

At steady state, the heating power supply to the resistance (Q_2) is equal to the sum of the heat losses (Q_{loss}) through the cup wall, heat exchange by convection from the liquid surface to the surrounding air (Q_{conv}) and heat exchange by water evaporation (Q_{evap}).

$$Q_1 = Q_{loss}$$

$$Q_2 = Q_{loss} + Q_{conv} + Q_{evap}$$

$$Q_{conv} = h * A * (T_{liq} - T_{air})$$

$$Q_{evap} = \Delta m * \Delta h_{evap} / \Delta t$$

Q_1, Q_2, Q_{conv}, Q_{evap}: heat exchange (W)

A: liquid surface area (0.0038 m^2)

Δh_{evap}: latent heat of evaporation ($2.38.10^6$ J / kg)

Δt: duration of experiment with un-covered cup (2820s)

The convective heat transfer coefficient, h ($Wm^{-2}K^{-1}$) can be calculated as below:

$$h = \frac{Q_{conv}}{A(T_{liq} - T_{air})} = \frac{Q_2 - Q_1 - \Delta m \times \Delta h_{evap} / \Delta t}{A(T_{liq} - T_{air})} \quad (5)$$

It is to be reminded that for water at atmospheric pressure and for the temperature range used in our study (35 - 65°C), Δh_{evap} is considered to be constant ($2.38.10^6$ J/kg) because the variation is low in this temperature range ($2.35.10^6$ - $2.42.10^6$ J/kg).

III. Results and discussion

3.1. Analysis of airflow, heat and mass transfer above a cup of hot drink

As cited previously, the airflow and heat transfer above a cup of hot drink can be characterised by several dimensionless numbers. A drink cup can be considered as a truncated cylinder with the hot walls at the top and the side. Our first approach consists in a calculation of the order of magnitude of Re, Ra and Ri allowing the information on the flow regimes (laminar, turbulent) and the heat transfer mode (natural, forced and mixed convection). The following values were used to estimate the dimensionless numbers; for the room: air temperature 20°C, velocity 0.03 $m.s^{-1}$; for the cup: hot drink temperature 65°C, cup dimension 8cm diameter x 11cm height. The order of magnitude of the dimensionless number is presented in Table 1.

Taking into account this analysis based on the dimensionless numbers, the airflow, heat and vapour exchange between the drink and the air is expected to be a result of the interaction of several phenomena. Considering the similarity with the flow along flat plate, since $Re < 5.10^5$ and according to Incropera and Dewitt (1990), the boundary layer at the top should remain laminar. In fact, the liquid/air interface is not at the top of the cup, so that the vortices could appear behind the upper part of the cup wall. Considering the similarity to a partially hollow cylinder in our case, since $Re \geq 90$, Karmann vortex detachment is expected. According to Rayleigh and Richardson numbers, natural convection is a determinant effect. So, to summarised, there is an upward warm air flow from the drink surface and this air is replaced by cooler air flowing downward from the ambient. There is instable airflow with vortex shedding behind the cup. Additionally, water evaporates from the surface which contributes to upward gas motion. The natural convection related to the temperature difference between the hot drink and air should be more significant than the forced convection.

With the cup of vegetable oil at 20°C, the airflow modification is only due to the presence of an obstacle. In the case of vegetable oil at 65°C, the difference of airflows compared to the

one at 20°C is related to the heat exchange by natural convection. This exchange is influenced by the temperature difference between oil and air in the work zone. In the case of hot water at 65°C, the airflow is related to the combined heat exchange by convection and evaporation. This evaporation can significantly contribute to the vertical velocity component at the surface of the liquid.

3.2. Visualisation of airflow

The images of airflow above the cup filled with water (65°C) at 3 different moments are shown in Figure 5. The heating resistance cable can be seen on the bottom right of these images. The air flows upward because of water evaporation and the flow is oriented to the right side because of air extraction by fans. It can be observed the unsteady flow with vortices formation. From these images, pulse volatile aroma releases can be expected because the plumes and vortices transport them from the liquid surface to the air.

3.3. Influence of convection and evaporation on airflow

The mean (time –averaged) velocity field calculated from 700 couple of images is presented in Fig. 6 for 3 different cases: oil at 20°C, oil at 65°C and water at 65°C. The mean field is used to facilitate the comparison of different situations in spite that it gives incomplete information. The instantaneous field for given conditions can be significantly different but they correspond to too large amount of information.

The cup of oil at 20°C (Fig. 6a) shows the influence of obstacle on airflow. In this case, air flows above the cup with acceleration, first upward (at left) then downward (at right). Just above the liquid surface inside the cup, there is an air recirculation. The recirculation above obstacle was also observed by Martinuzzi and Tropea (1996).

For the cup of oil at 65°C (Fig. 6b), air recirculation just above the liquid surface is observed as in the case of oil at 20°C. In this case, one can expect that air flows upward along the cup by natural convection. This can explain why no downward airflow was observed in this case at right.

For the cup of water at 65°C (Fig. 6c), the air recirculation just above the liquid surface disappears while the upward flow is more noticeable.

Three profiles of horizontal (v_x, main air flow direction) and vertical velocity (v_y) were extracted from the mean air velocity field along a vertical line above the cup and just downstream (x=68.5 mm). The results are shown in Fig.7.

All values of horizontal velocity v_x are positive (Fig.7a), this means that air flows in the horizontal direction from the left to the right. v_x decreases form y=0 to $y \approx 5\text{cm}$, this represents the zone of influence of the obstacle. Airflow is less disturbed by the presence of the cup for y > 5cm. The v_x profiles are similar for the 3 cases: oil (20°C), oil (65°C), water (65°C).

The vertical velocity profiles v_y are quite different (Fig. 7b). Only the case of oil at 20°C shows negative velocity for $0 < y < 4$ cm. This is a result of downward airflow behind the cup after the flow above it. When the temperature of the liquid is higher than the one of upstream air, air flows upward because of the effect of natural convection. This effect is more significant for evaporable liquid.

3.4. Influence of water temperature on airflow

The mean air velocity field for cup filled with water at 35°C, 45°C, 55°C and 65°C is shown in Fig. 8. The effect of water temperature on the airflow pattern (upward flow) becomes really

309 significant when temperature is higher than 55°C. This can be explained by the non linearity
310 between saturated pressure of water and its temperature. Indeed, at 35°C, for example, the
311 saturation vapour pressure is only about 6 kPa, that means that at the liquid/air interface water
312 vapour represents only 6% of the molar fraction. Therefore the evaporation effect is small.
313 Increasing the temperature from 35°C to 45°C increases the vapour fraction by only 4%. At
314 55°C, the vapour fraction becomes about 16% and a slight modification of flow pattern can be
315 observed. At 65°C, water vapour represents 25% of molar fraction at the liquid/air interface.
316 The evaporation effect becomes obvious. The natural convection effect is due partly to the
317 temperature difference $\Delta\rho/\rho \approx \Delta T/T \approx 7\%$ and partly to molar weight
318 difference $\Delta\rho/\rho \approx x(M_{air} - M_{water})/M_{air} \approx 10\%$ $(M_{air} = 29\,g/mol, M_{water} = 18\,g/mol)$. From
319 the flow pattern at 65°C, it can be expected that aroma compounds can be entrained
320 efficiently by the evaporated water.

321 **3.5. Air temperature and velocity fluctuations**

322 The air temperature measured every second for y=5, 10, 20, 30 and 40mm and x=68.5 mm is
323 presented in Fig. 9 for the cups of oil and water at 65°C. The same variation cycles can be
324 observed for every position. This figure also shows the air velocity magnitude extracted from
325 20 PIV images measured every 0.25s, fluctuations are also observed. This is because of the
326 strong relation between air temperature and velocity when natural convection is the dominant
327 heat transfer mode.

328 The mean and standard deviation of temperature (3600 measurements, duration 3600s) and
329 velocity (800 measurements, duration 200s) are reported in Table 2. For both cases (oil and
330 water), the air temperature decreases with the height (y) while the air velocity increases.

331 The difference of temperature fluctuations for the cups of oil and water can be explained by
332 the difference of involved phenomena. The main heat exchange for the cup of oil is natural

convection. For the cup of water, the combined natural convection and water evaporation leads to the intermittent detachment of hot and humid air plumes above it. The upward flow of hot and humid air is balanced by the downward flow of cold and dry ambient air. This explains the more temperature variations with time and the higher temperature decrease with the height for the water cup.

For an isothermal flow around an infinite cylinder of the same diameter as the cup, ($Re_D = 150$, see Table 1), Strouhal number is about 0.18 and the frequency of vortex shedding of 0.07 Hz is estimated. This frequency is in the range of the observed fluctuations of several seconds. But the interaction with the detachment of the plumes (due to the combined natural convection and evaporation) and the airflow near the upper surface made certainly the phenomena more complex and un-periodic. It is to be emphasized that a Fourier Transform was carried out; however, no specific frequency could be identified. This means that these fluctuations are rather random.

3.6. Heat transfer coefficient between air and water

The experimental values of the heat flux (Q) are shown in Table 3. Without evaporation, the convective heat transfer coefficient at the liquid/air interface is 18.7 $W.m^{-2}K^{-1}$ (cup of oil at 65°C). For laminar flow over an isothermal horizontal flat plate, heat transfer coefficients by natural and forced convection of 6.7 and 7.4 $W.m^{-2}.K^{-1}$ were obtained respectively (calculation based on the equations 1 and 3 and for D = 8 cm). The experimental value is almost equal to the sum of these values. For the cup of water at 65°C, it can be observed that the heat flux due to the latent heat of evaporation (Q_{evap}) is more than 3 times higher than the convective flux. The presence of evaporation enhance also the convective flux, the heat transfer coefficient is indeed increased from 18.7 to 24.9 $W.m^{-2}K^{-1}$.

The air velocity due to evaporative airflow is about 0.003 $m.s^{-1}$. This estimation is based on the weight loss during the experiment of the cup filled with water ($v = \frac{\Delta m}{\Delta t \rho A}$).

From these results, the cooling rate of a well-insulated cup of hot drink or of a non-insulated cup can be estimated. In the first case, the heat loss is only by convection and evaporation at the top (liquid/air interface, $h \approx 25$ $Wm^{-2}K^{-1}$, cf. Table 3), the heat loss is about 6W and the cooling rate about 0.35°C/min. In the second case, there are also heat losses through the side walls ($h \approx 10$ $Wm^{-2}K^{-1}$) and the cooling rate is about 1°C/min.

4. Conclusion

An attempt was carried out in this study to understand the mechanism of airflow above the cup with the objective to have a quantitative heat and mass transfer analysis and to gain knowledge which will be transposable to indoor aroma compound dispersion in relation with the ambient smell perceived by consumer. The airflow measurement by PIV over the cup filled with hot water shows that the flow is unsteady with vortex formation. This suggests pulsative release of aroma compounds from a hot drink. The air velocity varies both due to the position and the time. This complexity is related to the instantaneous heat exchanges by convection and evaporation between the water and surrounding air coupled with the unsteady flow expected behind the cup.

An experimental methodology was developed to determine the heat transfer coefficient between a cup of hot drink and ambient air. This parameter allows the prediction of the cooling rate of a drink in room condition.

ACKNOWLEDGEMENTS

The authors thank Daniel Picque, David Leveque and Jerome Bussière for their help in the construction of the device allowing temperature and air velocity in controlled conditions.

They also thank Gail Wagman for her precious help in revising the English.

References

Alamyane A.A. and Mohamad A.A., 2010. Simulation of forced convection in a channel with extended surfaces by the lattice Boltzmann method. *Computers and Mathematics with Applications*, 59, 2421-2430.

Carey, M.E., Asquith, T., Linforth, R.S.T., Taylor, A.J., 2002. Modeling the partition of volatile aroma compounds from a cloud emulsion. *Journal of Agricultural and Food Chemistry,* 50, 1985–1990.

Chyu M.K. and Natarajan V., 1996. Heat transfer on the base surface of three dimensional protruding elements. *International Journal Heat and Mass Transfer*, 39, 2925-2935.

Deleris I., Zouid I., Souchon I., Tréléa I.C., 2009. Calculation of apparent diffusion coefficients of aroma compounds in dairy emulsions based on fat content and physicochemical properties in each phase. *Journal of Food Engineering*, 94, 205–214.

Incropera F.P. and Dewitt D.P., 1990. Fundamentals of Heat and Mass Transfer. New York: Wiley.

Doulia, D., Tzia, K., Gekas, V., 2000. A knowledge base for the apparent mass diffusion coefficient (DEFF) in foods. *International Journal of Food Properties.* 3 (1), 1–14.

Doyen, K., Carey, M.E., Linforth, R.S.T., Marin, M., Taylor, A.J., 2001. Volatile release from an emulsion: headspace and in-mouth studies. *Journal of Agricultural and Food Chemistry*, 49 (2), 804–810.

Giroux, H.J., Perreault, V., Britten, M., 2007. Characterization of hydrophobic flavour release profile in oil-in-water emulsions. *Journal of Food Science*, 72 (2), S125–S129.

Hall C. W., 2000. Laws and Models: Science, Engineering and Technology, Boca Raton, CRC Press, 524 p.

Incropera F.P. and DeWitt D.P., 1996. *Fundamentals of Heat and Mass Transfer*, John Wiley & Sons, INC. 4ème edition, New York, Chapter 6 and 9, 886 p.

Jubran B.A., Swiety S.A., Hamdan M.A., 1996. Convective heat transfer and pressure drop characteristics of various array configurations to simulate the cooling of electronic equipment, *International Journal Heat and Mass Transfer*, 39, 3519-3529.

Landy, P., Rogacheva, S., Lorient, D., Voilley, A., 1998. Thermodynamic and kinetic aspects of the transport of small molecules in dispersed systems. *Colloids and Surfaces Biointerfaces*, 12, 57–65.

Mamun, M.A.H., Rahman M.M., Billah M.M., Saidur R., 2010. A numerical study on the effect of a heated hollow cylinder on mixed convection in a ventilated cavity, *International Communications in Heat and Mass Transfer*, 37, 1326-1334.

Marin M, Baek I, Taylor A.J., 1999. Volatile release from aqueous solutions under dynamic headspace dilution conditions, *Journal of Agricultural and Food Chemistry*, 47(11), 4750-4755.

Martinuzzi R., Tropea C., 1996. The flow around surfaced-mounted, prismatic obstacles placed in a fully developed channel flow, *Journal Fluids Engineering,* 115, 85-92.

Meynier, A., Lecoq, C., Genot, C., 2005. Emulsification enhances the retention of esters and aldehydes to a greater extent than changes in the droplet size distribution of the emulsion. *Food Chemistry,* 93 (1), 153–159.

Moussaoui M.A., Jami M., Mezrhab A., Naji H., 2010. MRT-Lattice Boltzmann simulation of forced convection in a plane channel with an inclined square cylinder, *International Journal of Thermal Sciences*, 49, 131-142.

Plana-Fattori A., Trelea I.C., Le Page J.F., Souchon I., Pollien P., Ali S., Ramaioli M., Pionnier-Pineau E., Hartmann C., Flick D., 2014. A novel approach for studying the indoor

427 dispersion of aroma through computational fluid dynamics, *Flavour and Fragrance Journal*,
428 29 (3), 143-156.

429 Philippe, E., Seuvre, A.M., Colas, B., Langendorff, V., Schippa, C., Voilley, A., 2003.
430 Behavior of flavor compounds in model food systems: a thermodynamic study. *Journal of*
431 *Agricultural and Food Chemistry,* 51, 1393–1398.

432 Rabe, S., Krings, U., Berger, R.G., 2004. Dynamic flavour release from miglyol/water
433 emulsions: modelling and validation. *Food Chemistry,* 84 (1), 117–125.

434 Rahman, M.M., Alim, M.A., Saha, S., Chowdhury, M.K., 2008. Mixed convection in a vented
435 square cavity with a heat conducting horizontal solid circular cylinder, *J. Nav. Arch. Mar.*
436 *Eng*, 5 (2) 37–46.

437 Rahman, M.M., Alim, M.A., Mamun M.A.H., 2009. Finite element analysis of mixed
438 convection in a rectangular cavity with a heat-conducting horizontal circular cylinder,
439 *Nonlinear analysis, Model. Control* 14 (2) 217–247.

440 Relkin, P., Fabre, M., Guichard, E., 2004. Effect of fat nature and aroma compound
441 hydrophobicity on flavor release from complex food emulsions. *Journal of Agricultural and*
442 *Food Chemistry*, 52 (20), 6257–6263.

443 Roberts, D.D., Pollien, P., Antille, N., Lindinger, W., Yeretzian, C., 2003. Comparison of
444 nosespace, headspace, and sensory intensity ratings for the evaluation of flavour absorption
445 by fat. *Journal of Agricultural and Food Chemistry,* 51 (12), 3636–3642.

446 Overbosch, P., Afterof, W.G.M., Haring, P.G.M., 1991. Flavor release in the mouth, *Food*
447 *Reviews International*, 7 (2) 137-184.

448 Shah K., Ferizer J.H., 1997, A fluid mechanicians view of wind engineering: Large eddy
449 simulation of flow past a cubic obstacle, *Journal of Wind Engineering and Industrial*
450 *Aerodynamics*, 67-68, 211-224.

451 Sparrow E.M., Niethammer J.E., Chaboki A., 1982. Heat transfer and pressure drop
452 characteristics of arrays of rectangular modules encountered in electronic equipment.
453 *International Journal Heat and Mass Transfer*, 25, 961-973.

454 Sparrow E.M., Yanezmoreno A.A., Otis D.R., 1984. Convective heat transfer response to
455 height differences in an array of block like electronic components. *International Journal Heat*
456 *and Mass Transfer*, 27, 469-473.

457 Stroebele N, De Castro JM., 2004. Effect of ambience on food intake and food choice.
458 *Nutrition*, 20(9) 821-38.

459 Taylor, A.J., Linforth, R.S.T., 1996. Flavour release in the mouth. *Trends in Food Science*
460 *and Technology,* 7 (12), 444–448.

461 Yong T.J. and Vafai K., 1998. Convective cooling of a heated obstacle in a channel,
462 *International Journal Heat and Mass Transfer*, 41, 3131-3148.

463 Wietrzak A. and Poulikakos D., 1990. Turbulent forced convective cooling of microelectronic
464 devices, *International Journal Heat and Mass Transfer*, 11, 105-113.

465

466

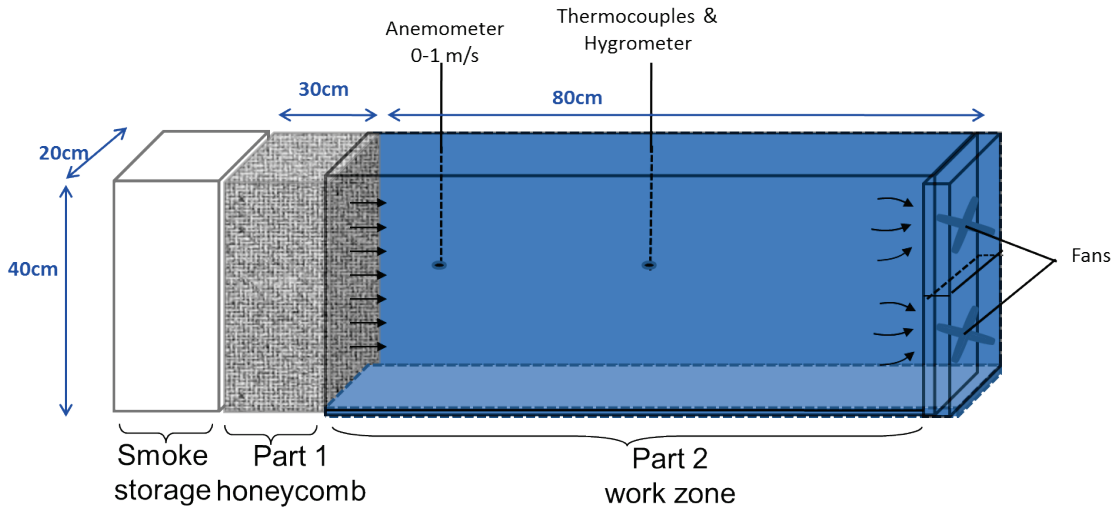

Figure 1: Experimental device

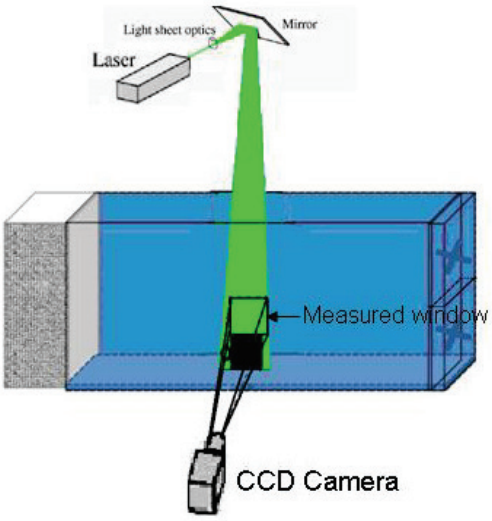

Figure 2: Position of laser beam, camera and measured window.

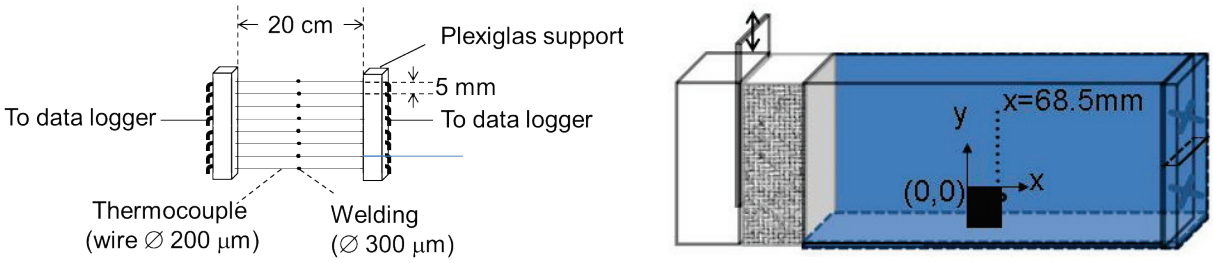

(a) (b)

Figure 3: a-Fixation device of 8 fine thermocouples (front view) b-Position of air temperature measurement above the cup.

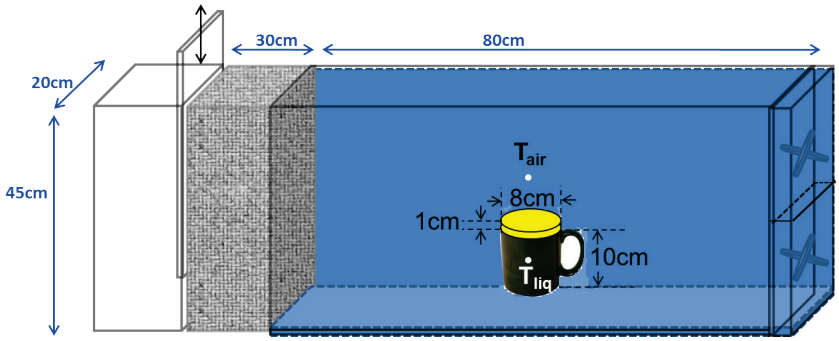

(a)

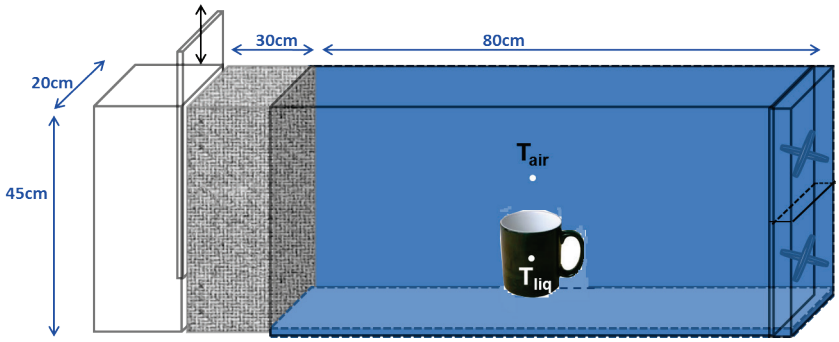

(b)

Figure 4: Heat transfer coefficient measurement

(a)- Cup covered with insulating plate (b)- Un-covered cup

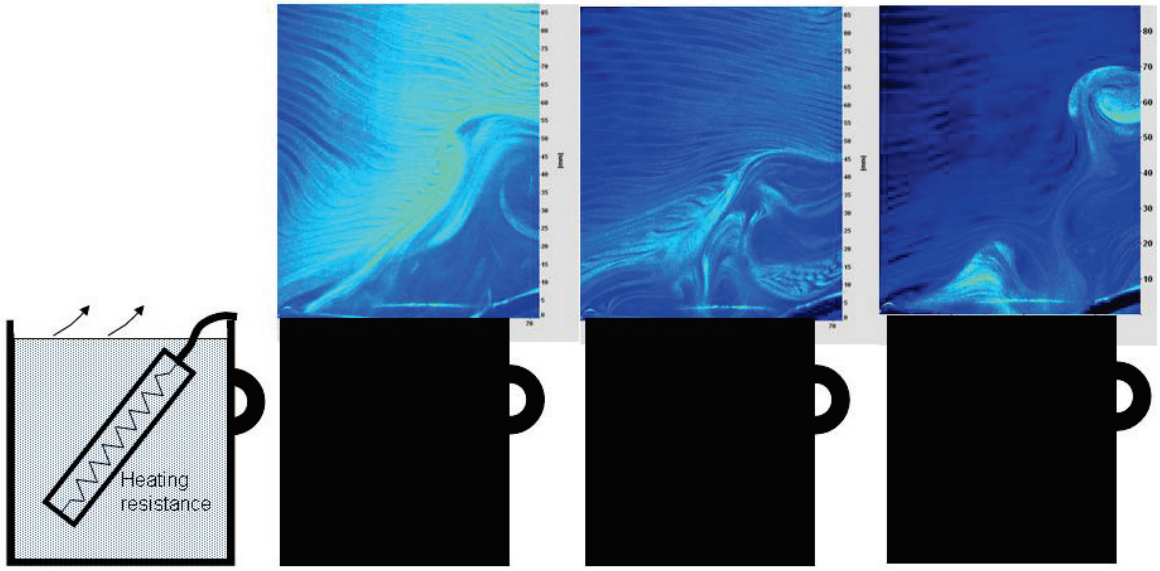

Figure 5: Images of airflow above the cup filled with water (65°C) at 3 different moments.

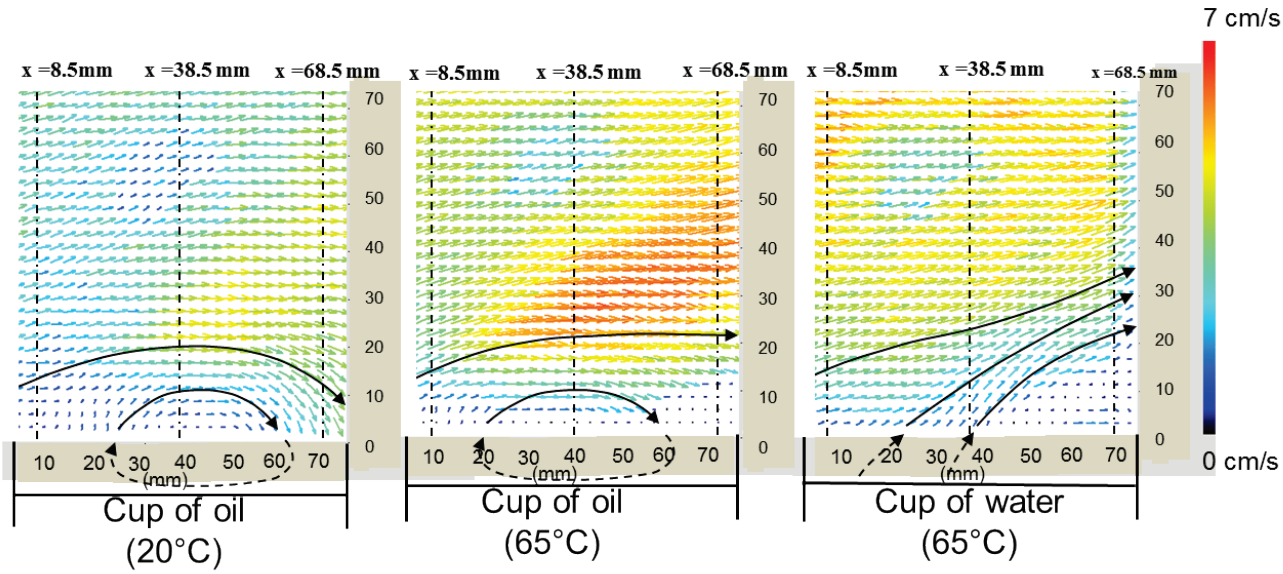

(a) (b) (c)

Figure 6: Mean air velocity field (mean of 700 measurements) above the cup filled with (a)- vegetable oil at 20°C (b)- vegetable oil at 65°C (c)- water at 65°C. Solid black lines represent the flow direction.

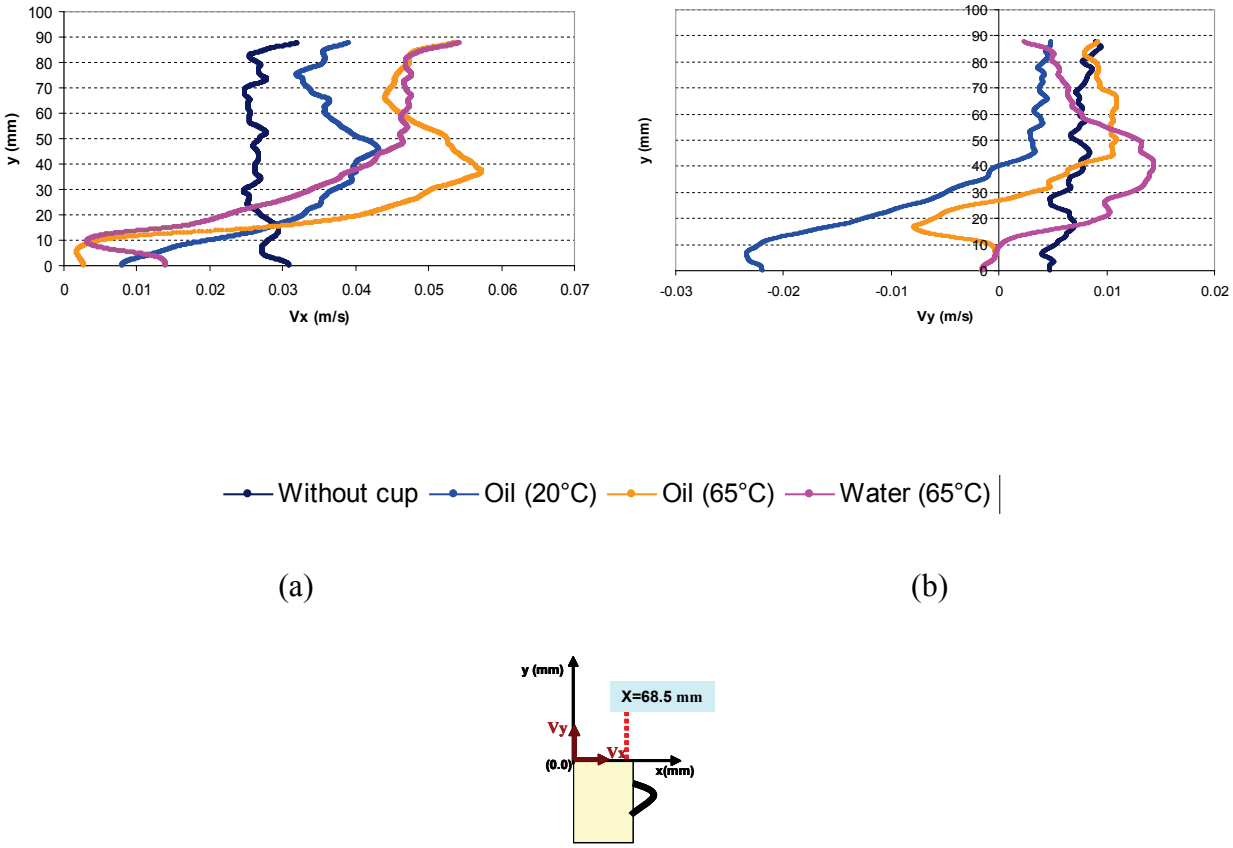

Figure 7: Mean air velocity at x=68.5 mm for the device without cup, cup filled with oil at 20°C, oil at 65°C and water at 65°C (a)- horizontal velocity, v_x (b)- vertical velocity, v_y.

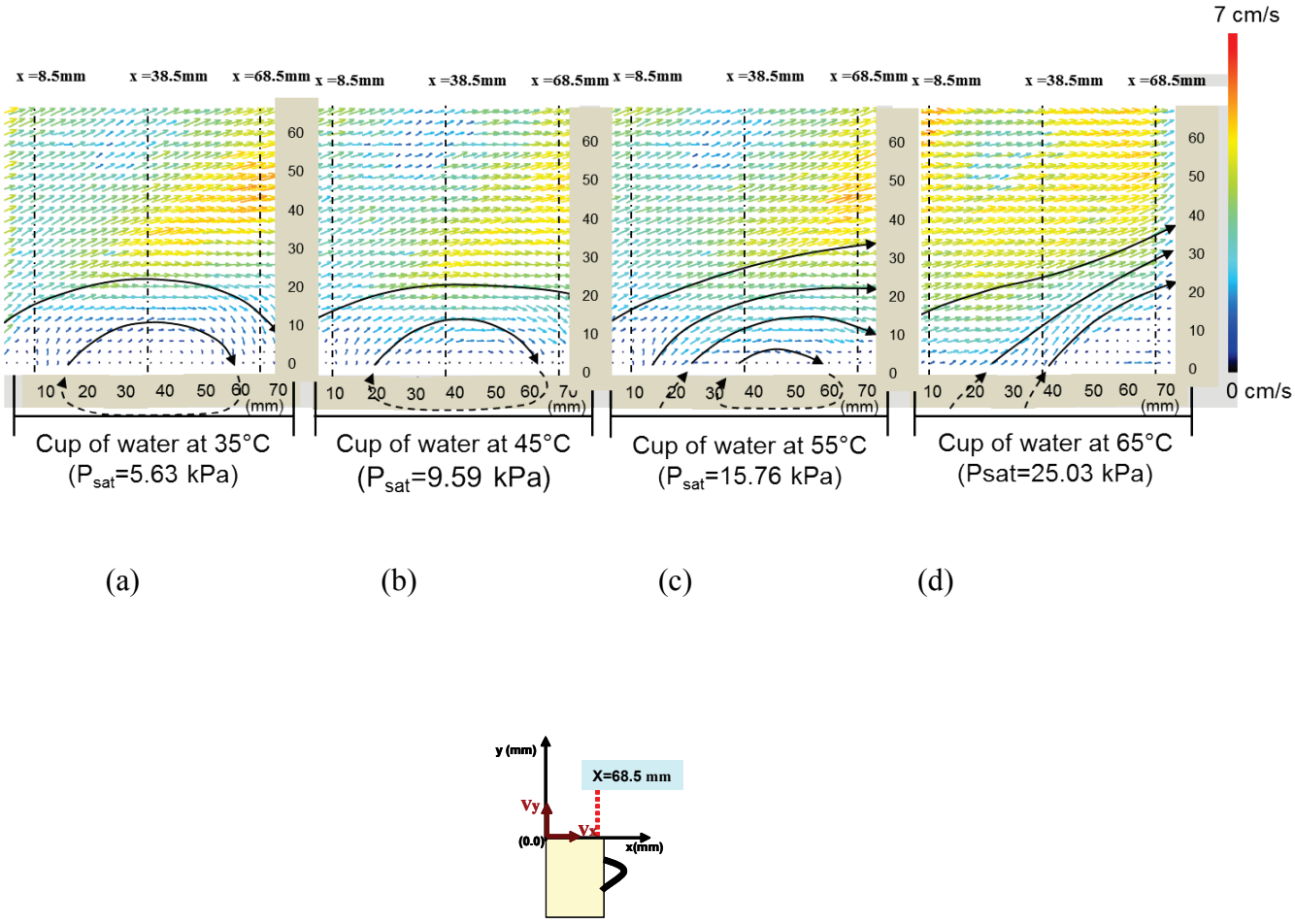

Figure 8: Mean air velocity field above the cup filled with water at different temperatures (a) 35°C (b) 45°C (c) 55°C (d) 65°C. Solid black lines represent the flow direction.

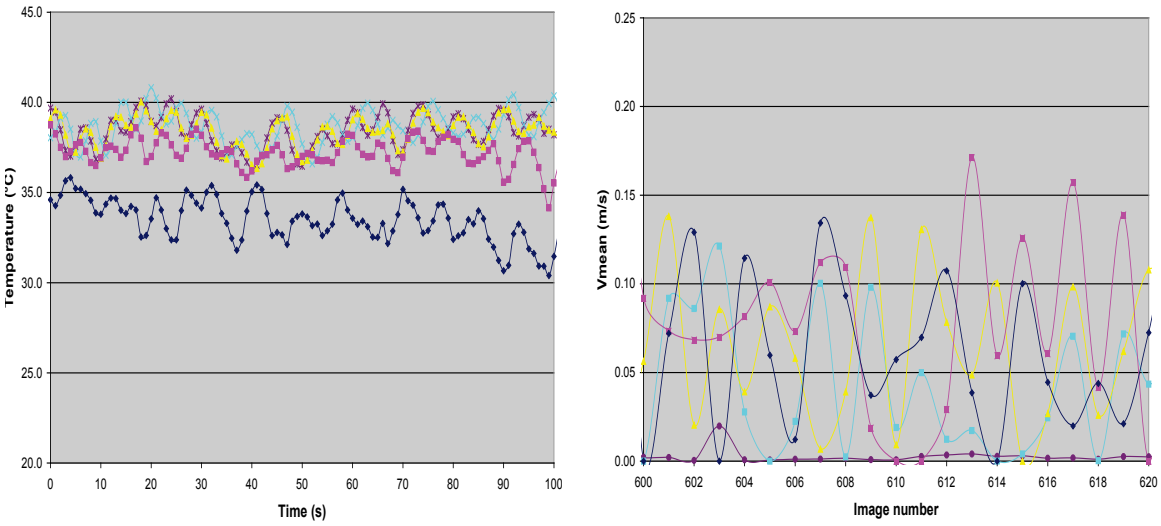

a-Cup of oil (65°C)

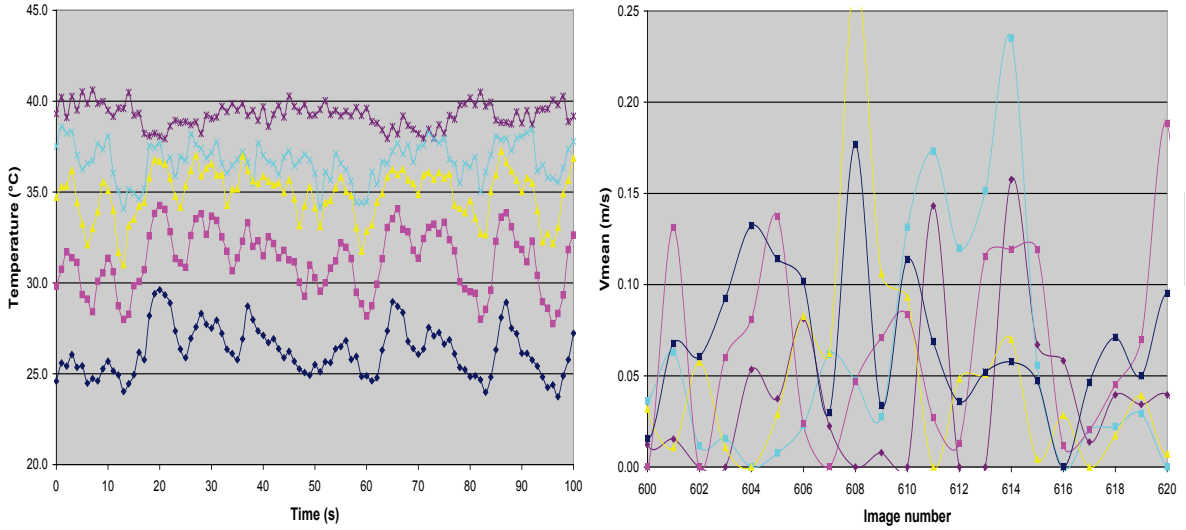

b-Cup of water (65°C)

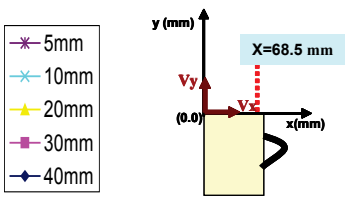

Figure 9: Air temperature fluctuations at y=5, 10, 20, 30 and 40mm for x=68.5 mm and air velocity magnitude measured every 0.25s.

Table 1: Order of magnitude of dimensionless numbers for a cup of hot drink placed in a room.

Dimensionless number	Value	Interpretation
Re_D	150	$Re \leq 5.10^5$, laminar airflow over the hot drink cup
		$Re \geq 90$, Karman vortex street downstream of the cylinder (unsteady-oscillating vortices).
Ra_D	$2.1x10^6$	$10^4 \leq Ra \leq 10^7$, laminar airflow by natural convection over the hot drink cup
Ri	124	Ri>10, natural convection between the drink and the surrounding air is the dominant heat transfer mode.

Table 2: Mean and standard deviation of air temperature and velocity at various heights (y) for x=68.5cm.

y (mm)	Cup of oil (65°C)				Cup of water (65°C)			
	Temperature (°C)		Velocity magnitude(m/s)		Temperature (°C)		Velocity magnitude(m/s)	
	Mean	Std	Mean	Std	Mean	Std	Mean	Std
5	38.43	0.94	0.0043	0.0103	39.24	0.65	0.0396	0.0430
10	38.68	0.93	0.0481	0.0515	36.73	1.04	0.0529	0.0517
20	38.40	0.83	0.0668	0.0576	34.89	1.35	0.0539	0.0535
30	37.20	0.77	0.0732	0.0566	31.23	1.68	0.0619	0.0539
40	33.47	1.19	0.0732	0.0520	26.24	1.36	0.0663	0.0546

Table 3: Convective heat transfer coefficient between oil-air and water-air.

Parameter	Convection (cup filled with oil at 65°C)	Convection+ evaporation (cup filled with water at 65°C)
Q_{Conv}/A ($W.m^{-2}$)	795	1099
Q_{Evap}/A ($W.m^{-2}$)	0	3547
$\Delta m/\Delta t$ (kg/s)	0	5.73×10^{-6}
h ($W.m^{-2}.K^{-1}$)	18.7	24.9